

**Yukawa corrections to  $\gamma\gamma \rightarrow b\bar{b}$  in the topcolor assisted technicolor models**Jinshu Huang<sup>1,2,\*</sup> and Gongru Lu<sup>1,+</sup><sup>1</sup>*Department of Physics, Henan Normal University, Xinxiang 453007, People's Republic of China*<sup>2</sup>*Department of Physics, Nanyang Normal University, Nanyang 473061, People's Republic of China*

(Received 5 May 2008; published 15 August 2008)

We study the Yukawa corrections to the  $\gamma\gamma \rightarrow b\bar{b}$  cross section in the topcolor assisted technicolor models at the photon-photon colliders. We find that, for the favorable parameters, the relative corrections from pseudo-Goldstone bosons give out a 3.2% ~ 5.9% decrement of the cross section from the tree level when  $\sqrt{s} = 500$  GeV, the contributions from new extended technicolor gauge bosons  $Z^*$  and colored gauge bosons  $B$  are negligibly small, and the relative correction arising from new color-singlet heavy gauge boson  $Z'$  is less than -3.2%. Therefore, the total relative corrections are significantly larger than the corresponding corrections in the standard model, the general two Higgs doublet model, and the minimal supersymmetric standard model. Since these corrections are obvious for the International Linear Colliders, the process  $\gamma\gamma \rightarrow b\bar{b}$  is really interesting in testing the standard model and searching for the signs of technicolor.

DOI: [10.1103/PhysRevD.78.035007](https://doi.org/10.1103/PhysRevD.78.035007)

PACS numbers: 12.60.Nz, 12.38.Bx, 14.65.Fy

**I. INTRODUCTION**

The collisions of high energy photons produced at the linear collider provide a comprehensive laboratory for testing the standard model (SM) and probing new physics beyond the SM [1]. With the advent of the new collider technique [2], one can obtain the high energy and high intensity photon beams by using Compton laser photons scattering off the colliding electron and positron beams, and a large number of heavy quark pairs can be produced by this method. The photon energy spectrums show that there are many relatively soft photons, and the production of heavy top quarks will be suppressed for reduced collision energies, but no such suppression affects the relatively light bottom quarks [3]. Therefore it is worthy to investigate the production of the bottom quark pairs in the photon-photon collisions.

In the SM, this process has been calculated and the QCD threshold effects of the process also have been examined [4]. Reference [5] has investigated the Yukawa corrections to this process in both the general two Higgs doublet model (2HDM) and the minimal supersymmetric standard model (MSSM), which shows the relative corrections to the total cross section of the process  $e^+e^- \rightarrow \gamma\gamma \rightarrow b\bar{b}$  are less than 0.1% for favorable parameter values. In the paper, we present the calculation of the Yukawa corrections to this process in the topcolor assisted technicolor models, which arise from the virtual effects of the third-generation quarks, charged pseudo-Goldstone bosons (PGBs), and new gauge bosons in photon-photon collisions. It is organized as follows. In Sec. II, we present a brief review of the original topcolor assisted technicolor (TOPCTC) model and the multiscale walking topcolor assisted technicolor

(TOPCMTC) model. In Sec. III, we give out the analytical results in terms of the well-known standard notation of one-loop Feynman integrals. The numerical results and conclusions are included in Sec. IV, and the form factors appearing in the cross section are presented in the Appendices A and B.

**II. GENERAL CHARACTERISTICS OF THE TOPCOLOR ASSISTED TECHNICOLOR MODELS**

As we know, technicolor—a strong interaction of fermions and gauge bosons at the scale  $\Lambda_{\text{TC}} \sim 1$  TeV—is a scenario for the dynamical breakdown of electroweak symmetry to electromagnetism [6]. Based on the similar phenomenon of chiral symmetry breakdown in QCD, technicolor is explicitly defined and completely natural. To account for the mass of quarks, leptons, and Goldstone “technipions” in such a scheme, technicolor, ordinary color, and flavor symmetry are embedded in a large gauge group, called extended technicolor (ETC) [7]. Because of the conflict between constraints on flavor-changing neutral currents and the magnitude of ETC-generated quark, lepton, and technipion masses, classical technicolor was superseded by a “walking” technicolor and “multiscale technicolor” [8,9]. The incapability of explaining the top quark’s large mass without a clash of either cherished notions of naturalness or experiments from the  $\rho$  parameter and the  $Z \rightarrow b\bar{b}$  decay rate by ETC [10] led to the original topcolor assisted technicolor by C. T. Hill [11] and the multiscale walking topcolor assisted technicolor model [12].

The original TOPCTC model assumes [11,13,14]: (i) electroweak interactions are broken by technicolor; (ii) the top quark mass is large because it is the combination of a dynamical condensate component  $(1 - \epsilon)m_t$ , generated by a new strong dynamics, together with a small

\*jshuang@vip.sina.com

+lugongru@sina.com

fundamental component  $\varepsilon m_t$  ( $\varepsilon \sim 0.03\text{--}0.1$ ), generated by ETC; (iii) the new strong dynamics is assumed to be chiral critically strong but spontaneously broken by technicolor at the scale  $\sim 1$  TeV, and it generally couples preferentially to the third generation. This needs a new class of technicolor models incorporating ‘‘topcolor’’ (TOPC). The dynamics at  $\sim 1$  TeV scale involves the gauge structure

$$\begin{aligned} & SU(3)_1 \times SU(3)_2 \times U(1)_{Y_1} \times U(1)_{Y_2} \\ & \rightarrow SU(3)_{\text{QCD}} \times U(1)_{\text{EM}} \end{aligned} \quad (1)$$

where  $SU(3)_1 \times U(1)_{Y_1} [SU(3)_2 \times U(1)_{Y_2}]$  generally couples preferentially to the third (first and second) generation, and is assumed to be strong enough to form chiral  $\langle \bar{t}t \rangle$  but not  $\langle \bar{b}b \rangle$  condensation by the  $U(1)_{Y_1}$  coupling. A residual global symmetry  $SU(3)' \times U(1)'$  implies the existence of a massive color-singlet heavy  $Z'$  and an octet  $B$ . A symmetry-breaking pattern outlined above will generically give rise to three top pions,  $\pi_t$ , near the top mass scale.

The couplings of gauge bosons  $Z'$  and  $B$  to bottom quark given by the topcolor interactions which for the process  $\gamma\gamma \rightarrow b\bar{b}$  can be written as

$$Z'b\bar{b}: \frac{1}{6}g_1 \cot\theta' \gamma^\mu L - \frac{1}{3}g_1 \cot\theta' \gamma^\mu R, \quad (2)$$

$$Bb\bar{b}: \frac{1}{2}g_3 \cot\theta \lambda^a \gamma^\mu, \quad (3)$$

where  $L, R = (1 \mp \gamma_5)/2$  are the left- and right-handed projectors,  $\lambda^a$  is a Gell-Mann matrix acting on ordinary color indices,  $g_3$  ( $g_1$ ) is the QCD  $U(1)_Y$  coupling constant at the scale  $\sim 1$  TeV. The SM  $U(1)_Y$  field  $B_\mu$  and the  $U(1)'$  field  $Z'_\mu$  are then defined by orthogonal rotation with mixing angle  $\theta$  ( $\theta'$ ). If we take

$$\kappa = \frac{g_3^2 \cot^2 \theta}{4\pi}, \quad \kappa_1 = \frac{g_1^2 \cot^2 \theta'}{4\pi}, \quad (4)$$

Ref. [15] shows that the value of  $\kappa$  must be approximately 2 and  $\kappa_1$  is assumed to be  $O(1)$ .

There exist the ETC gauge bosons  $Z^*$  including the sideways and diagonal gauge bosons in this model. The coupling of  $Z^*$  to the fermions and technifermions can be found in Ref. [16]. For the sake of simplicity, we assume that the mass of the sideways gauge boson is equal to the mass of the diagonal gauge boson, namely  $m_{Z^*}$ , so the  $Z^*b\bar{b}$  coupling by the ETC dynamics can be given by

$$Z^*b\bar{b}: -\frac{\varepsilon m_t}{16\pi f_\pi} \frac{e}{s_W c_W} \left[ \frac{N_C}{N_{TC} + 1} \xi_t (\xi_t^{-1} + \xi_b) - \xi_t^2 \right] \gamma_\mu L, \quad (5)$$

where  $N_{TC}$  and  $N_C$  are the numbers of technicolors and ordinary colors, respectively;  $s_W = \sin\theta_W$  and  $c_W = \cos\theta_W$  with  $\theta_W$  being the Weinberg angle;  $\xi_t$  and  $\xi_b$  are coupling coefficients and are ETC gauge-group-

dependent. Following Ref. [16], we take  $\xi_t = 1/\sqrt{2}$  and  $\xi_b = 0.028\xi_t^{-1}$ .

In this TOPCTC model, there are 60 technipions in the ETC sector with decay constant  $f_\pi = 123$  GeV and three top pions  $\pi_t^0, \pi_t^\pm$  in the TOPC sector with decay constant  $f_{\pi_t} = 50$  GeV. The ETC sector is a one-generation technicolor model [7]. The relevant technipions in this study are only the color-singlet  $\pi$  and color-octet  $\pi_8$ . The color-singlet (octet) technipion-top (bottom) interactions are given by

$$\begin{aligned} & \frac{c_t \varepsilon m_t}{\sqrt{2} f_\pi} \left[ i\bar{t} \gamma_5 t \pi^0 + i\bar{t} \gamma_5 t \pi^3 + \frac{1}{\sqrt{2}} \bar{t} (1 - \gamma_5) b \pi^+ \right. \\ & \left. + \frac{1}{\sqrt{2}} \bar{b} (1 + \gamma_5) t \pi^- \right], \end{aligned} \quad (6)$$

$$\begin{aligned} & \frac{\sqrt{2} \varepsilon m_t}{f_\pi} \left[ i\bar{t} \gamma_5 \frac{\lambda^a}{2} t \pi_8^0 + i\bar{t} \gamma_5 \frac{\lambda^a}{2} t \pi_8^3 \right. \\ & \left. + \frac{1}{\sqrt{2}} \bar{t} (1 - \gamma_5) \frac{\lambda^a}{2} b \pi_8^+ + \frac{1}{\sqrt{2}} \bar{b} (1 + \gamma_5) \frac{\lambda^a}{2} t \pi_8^- \right], \end{aligned} \quad (7)$$

with the coefficient  $c_t = 1/\sqrt{6}$ .

The coupling of the top pions to the top (bottom) quark has the form

$$\begin{aligned} & \frac{(1 - \varepsilon) m_t}{\sqrt{2} f_{\pi_t}} \left[ i\bar{t} \gamma_5 t \pi_t^0 + \frac{1}{\sqrt{2}} \bar{t} (1 - \gamma_5) b \pi_t^+ \right. \\ & \left. + \frac{1}{\sqrt{2}} \bar{b} (1 + \gamma_5) t \pi_t^- \right]. \end{aligned} \quad (8)$$

The interaction of the gauge boson  $\gamma$  and the top pions  $\pi_t^\pm$  is

$$\frac{i}{2} g (p' - p)^\mu, \quad (9)$$

which  $p', p$  denote the momentums of  $\pi_t^+$  and  $\pi_t^-$ , respectively, and the coupling constant  $g$  is defined by  $g = e/\sin\theta_W$ . More detailed Feynman rules needed in the calculations can be found in Refs. [17,18].

For the topcolor assisted multiscale technicolor model [12,19], it is different from the original TOPCTC model mainly by the ETC sector. In the original TOPCTC model, the ETC sector is the one-generation technicolor model with  $f_\pi = 123$  GeV,  $c_t = 1/\sqrt{6}$ , and  $N_{TC} = 4$ ; and in the TOPCMTC model the ETC sector is the multiscale walking technicolor model with  $f_\pi = 40$  GeV,  $c_t = 2/\sqrt{6}$ , and  $N_{TC} = 6$  [12,19].

### III. YUKAWA CORRECTIONS TO THE BOTTOM PAIR PRODUCTION IN PHOTON-PHOTON COLLISIONS

The relevant Feynman diagrams for the corrections arising from PGBs to the  $\gamma\gamma \rightarrow b\bar{b}$  production amplitudes are shown in Figs. 1(c)–1(m). In our calculation, we use the

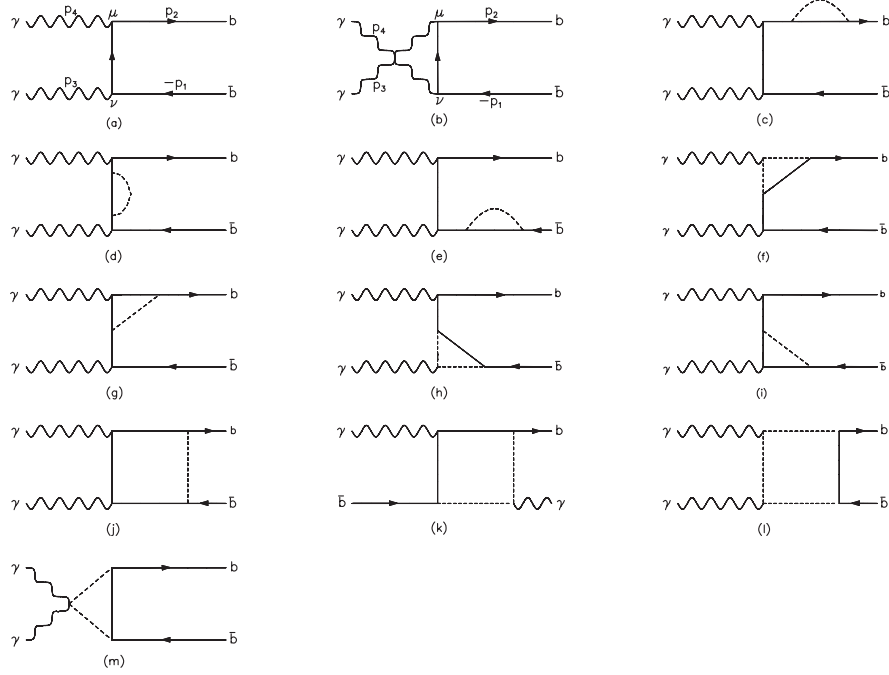


FIG. 1. Feynman diagrams for PGB contributions to the  $\gamma\gamma \rightarrow b\bar{b}$  process: (a)-(b) tree-level diagrams; (c)-(e) self-energy diagrams; (f)-(i) vertex diagrams; (j)-(l) box diagrams; (m) triangle diagram. Here only one-loop diagrams corresponding to the tree-level diagram (a) are plotted. The dashed lines represent the charged technipions  $\pi^\pm$ ,  $\pi_8^\pm$  and top pions  $\pi_t^\pm$  in the figures (c)-(m).

dimensional regularization to regulate all the ultraviolet divergences in the virtual loop corrections, and adopt the Feynman gauge and on-mass-shell renormalization scheme [20]. The renormalized amplitude for  $\gamma\gamma \rightarrow b\bar{b}$  contains

$$\begin{aligned} M_{\text{ren}} &= M_0 + \delta M \\ &= M_0 + \delta M^{\text{self}} + \delta M^{\text{vertex}} + \delta M^{\text{box}} + \delta M^{\text{tr}}, \end{aligned} \quad (10)$$

where  $M_0$  is the amplitude at the tree level;  $\delta M^{\text{self}}$ ,  $\delta M^{\text{vertex}}$ ,  $\delta M^{\text{box}}$ , and  $\delta M^{\text{tr}}$  represent the Yukawa corrections arising from the self-energy, vertex, box, and triangle diagrams, respectively. Their explicit forms are given by

$$M_0 = M_0^{\hat{t}} + M_0^{\hat{u}}, \quad (11)$$

$$\delta M^{\text{self}} = \delta M^{s(\hat{t})} + \delta M^{s(\hat{u})}, \quad (12)$$

$$\delta M^{\text{vertex}} = \delta M^{v(\hat{t})} + \delta M^{v(\hat{u})}, \quad (13)$$

$$\delta M^{\text{box}} = \delta M^{b(\hat{t})} + \delta M^{b(\hat{u})}, \quad (14)$$

where

$$\begin{aligned} M_0^{\hat{t}} &= -i \frac{e^2 Q_b^2}{\hat{t} - m_b^2} \epsilon_\mu(p_4) \epsilon_\nu(p_3) \bar{u}(p_2) \\ &\quad \times \gamma^\mu (\not{p}_2 - \not{p}_4 + m_b) \gamma^\nu v(p_1), \end{aligned} \quad (15)$$

$$M_0^{\hat{u}} = M_0^{\hat{t}}(p_3 \leftrightarrow p_4, \hat{t} \leftrightarrow \hat{u}), \quad (16)$$

$$\begin{aligned} \delta M^{s(\hat{t})} &= i \frac{e^2 Q_b^2}{(\hat{t} - m_b^2)^2} \epsilon_\mu(p_4) \epsilon_\nu(p_3) \bar{u}(p_2) \\ &\quad \times [f_1^{s(\hat{t})} \gamma^\mu \gamma^\nu + f_2^{s(\hat{t})} p_2^\mu \gamma^\nu + f_3^{s(\hat{t})} \not{p}_4 \gamma^\mu \gamma^\nu] \\ &\quad \times v(p_1), \end{aligned} \quad (17)$$

$$\delta M^{s(\hat{u})} = \delta M^{s(\hat{t})}(p_3 \leftrightarrow p_4, \hat{t} \leftrightarrow \hat{u}), \quad (18)$$

$$\begin{aligned} \delta M^{v(\hat{t})} &= -i \frac{e^2 Q_b}{\hat{t} - m_b^2} \epsilon_\mu(p_4) \epsilon_\nu(p_3) \bar{u}(p_2) \\ &\quad \times [f_1^{v(\hat{t})} \gamma^\mu \gamma^\nu + f_2^{v(\hat{t})} \gamma^\mu p_1^\nu + f_3^{v(\hat{t})} p_2^\mu \gamma^\nu \\ &\quad + f_4^{v(\hat{t})} p_2^\mu p_1^\nu + f_5^{v(\hat{t})} \not{p}_4 \gamma^\mu \gamma^\nu + f_6^{v(\hat{t})} \not{p}_4 \gamma^\mu p_1^\nu \\ &\quad + f_7^{v(\hat{t})} \not{p}_4 p_2^\mu \gamma^\nu] v(p_1), \end{aligned} \quad (19)$$

$$\delta M^{v(\hat{u})} = \delta M^{v(\hat{t})}(p_3 \leftrightarrow p_4, \hat{t} \leftrightarrow \hat{u}), \quad (20)$$

$$\begin{aligned}
 \delta M^{b(\hat{i})} = & -i \frac{e^2}{16\pi^2} \epsilon_\mu(p_4) \epsilon_\nu(p_3) \bar{u}(p_2) [f_1^{b(\hat{i})} \gamma^\mu \gamma^\nu + f_2^{b(\hat{i})} \gamma^\nu \gamma^\mu + f_3^{b(\hat{i})} \gamma^\mu p_1^\nu + f_4^{b(\hat{i})} p_1^\mu \gamma^\nu + f_5^{b(\hat{i})} \gamma^\mu p_2^\nu + f_6^{b(\hat{i})} p_2^\mu \gamma^\nu \\
 & + f_7^{b(\hat{i})} p_1^\mu p_1^\nu + f_8^{b(\hat{i})} p_1^\mu p_2^\nu + f_9^{b(\hat{i})} p_2^\mu p_1^\nu + f_{10}^{b(\hat{i})} p_2^\mu p_2^\nu + f_{11}^{b(\hat{i})} \not{p}_4 \gamma^\mu \gamma^\nu + f_{12}^{b(\hat{i})} \not{p}_4 \gamma^\nu \gamma^\mu + f_{13}^{b(\hat{i})} \not{p}_4 \gamma^\mu p_1^\nu \\
 & + f_{14}^{b(\hat{i})} \not{p}_4 p_1^\mu \gamma^\nu + f_{15}^{b(\hat{i})} \not{p}_4 \gamma^\mu p_2^\nu + f_{16}^{b(\hat{i})} \not{p}_4 p_2^\mu \gamma^\nu + f_{17}^{b(\hat{i})} \not{p}_4 p_1^\mu p_1^\nu + f_{18}^{b(\hat{i})} \not{p}_4 p_1^\mu p_2^\nu + f_{19}^{b(\hat{i})} \not{p}_4 p_2^\mu p_1^\nu \\
 & + f_{20}^{b(\hat{i})} \not{p}_4 p_2^\mu p_2^\nu] v(p_1), \tag{21}
 \end{aligned}$$

$$\delta M^{b(\hat{u})} = \delta M^{b(\hat{i})}(p_3 \leftrightarrow p_4, \hat{i} \leftrightarrow \hat{u}), \tag{22}$$

and

$$\delta M^{\text{tr}} = i \frac{e^2}{8\pi^2} f_1^{\text{tr}} g^{\mu\nu} \epsilon_\mu(p_4) \epsilon_\nu(p_3) \bar{u}(p_2) v(p_1). \tag{23}$$

Here  $\hat{i} = (p_4 - p_2)^2$ ,  $\hat{u} = (p_4 - p_1)^2$ ,  $p_3$ , and  $p_4$  denote the momentum of the two incoming photons, and  $p_2$  and  $p_1$  are the momentum of the outgoing bottom quark and its antiparticle.

The form factors  $f_i^{s(\hat{i})}$ ,  $f_i^{v(\hat{i})}$ ,  $f_i^{b(\hat{i})}$ , and  $f_i^{\text{tr}}$  are expressed in terms of two-, three- and four-point scalar integrals, and are presented in Appendix A. The basic two-, three-, and four-scalar integrals are given in Ref. [21]. It is easy to find that all the ultraviolet divergences cancel in the effective vertex.

For the new gauge bosons ( $Z^*$ ,  $Z'$ , and  $B$ ), we plot the relevant Feynman diagrams for the contributions arising from these particles to the  $\gamma\gamma \rightarrow b\bar{b}$  production amplitudes in Fig. 2. The form factors from these new gauge bosons are similar to those of PGBs, and are given in Appendix B.

The cross section of the subprocess  $\gamma\gamma \rightarrow b\bar{b}$  for the unpolarized photons is given by

$$\hat{\sigma}(\hat{s}) = \frac{N_C}{16\pi\hat{s}^2} \int_{\hat{i}^-}^{\hat{i}^+} d\hat{t} \sum_{\text{spins}} |M_{\text{ren}}(\hat{s}, \hat{t})|^2, \tag{24}$$

where

$$\hat{t}^\pm = \left(m_b^2 - \frac{1}{2}\hat{s}\right) \pm \frac{1}{2}\hat{s} \sqrt{1 - 4m_b^2/\hat{s}}. \tag{25}$$

The bar over the sum recalls averaging over initial spins and

$$\sum_{\text{spins}} |M_{\text{ren}}(\hat{s}, \hat{t})|^2 = \sum_{\text{spins}} |M_0|^2 + 2 \text{Re} \sum_{\text{spins}} M_0^\dagger \delta M. \tag{26}$$

The total cross section  $\sigma(s)$  for the bottom pair production in  $\gamma\gamma$  collisions can be obtained by folding the elementary cross section  $\sigma(\hat{s})$  for the subprocess  $\gamma\gamma \rightarrow b\bar{b}$  with the photon luminosity at the  $e^+e^-$  colliders given in Refs. [4,5], i.e.,

$$\sigma(s) = \int_{2m_b/\sqrt{s}}^{x_{\text{max}}} dz \frac{dL_{\gamma\gamma}}{dz} \hat{\sigma}(\hat{s})(\gamma\gamma \rightarrow b\bar{b} \text{ at } \hat{s} = z^2s), \tag{27}$$

where  $\sqrt{s}$  and  $\sqrt{\hat{s}}$  are the  $e^+e^-$  and  $\gamma\gamma$  center-of-mass energies, respectively, and  $dL_{\gamma\gamma}/dz$  is the photon luminosity, which can be expressed as

$$\frac{dL_{\gamma\gamma}}{dz} = 2z \int_{z^2/x_{\text{max}}}^{x_{\text{max}}} \frac{dx}{x} F_{\gamma/e}(x) F_{\gamma/e}(z^2/x). \tag{28}$$

For unpolarized initial electron and laser beams, the energy spectrum of the backscattered photon is given by [4,22]

$$\begin{aligned}
 F_{\gamma/e}(x) = & \frac{1}{D(\xi)} \left[ 1 - x + \frac{1}{1-x} - \frac{4x}{\xi(1-x)} \right. \\
 & \left. + \frac{4x^2}{\xi^2(1-x^2)} \right], \tag{29}
 \end{aligned}$$

with

$$D(\xi) = \left(1 - \frac{4}{\xi} - \frac{8}{\xi^2}\right) \ln(1 + \xi) + \frac{1}{2} + \frac{8}{\xi} - \frac{1}{2(1 + \xi)^2}, \tag{30}$$

where  $\xi = 4E_e E_0/m_e^2$  in which  $m_e$  and  $E_e$  denote the incident electron mass and energy, respectively,  $E_0$  denotes

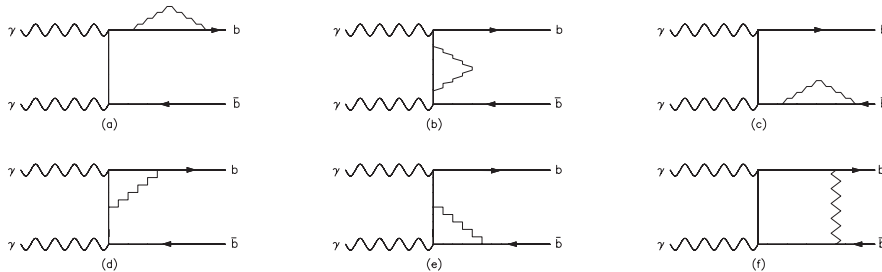


FIG. 2. Feynman diagrams for the contributions arising from new gauge bosons to the  $\gamma\gamma \rightarrow b\bar{b}$  process: (a)-(c) self-energy diagrams; (d)-(e) vertex diagrams; (f) box diagram. Here only one-loop diagrams corresponding to the tree-level  $t$ -channel diagram are plotted. The folding lines denote the new gauge bosons ( $Z^*$ ,  $Z'$ , and  $B$ ).

the initial laser photon energy, and  $x = E/E_e$  is the fraction which represents the ratio between the scattered photon and initial electron energy for the backscattered photons moving along the initial electron direction.  $F_{\gamma/e}(x)$  vanishes for  $x > x_{\max} = E_{\max}/E_e = \xi/(1 + \xi)$ . In order to avoid the creation of  $e^+e^-$  pairs by the interaction of the incident and backscattered photons, we require  $E_0 x_{\max} \leq m_e^2/E_e$ , which implies  $\xi \leq 2 + 2\sqrt{2} \approx 4.8$  [22]. For the choice  $\xi = 4.8$ , it can obtain

$$x_{\max} \approx 0.83, \quad D(\xi) \approx 1.8. \quad (31)$$

## IV. NUMERICAL RESULTS AND CONCLUSIONS

### A. The PGBs contributions

It is necessary to point out that, in the calculation of  $\hat{\sigma}(\hat{s})$ , instead of calculating the square of the amplitude  $M_{\text{ren}}$  analytically, we calculate the amplitudes numerically by using the method of Ref. [23]. Care must be taken in the calculation of the form factors expressed in terms of the standard loop integrals. As has been discussed in Ref. [24], the formulas for the form factors given in terms of the tensor loop integrals will be ill-defined when the scattering is forward or backward wherein the Gram determinants of some vanish and thus their inverses do not exist. This problem can be solved by taking kinematic cuts on the rapidity  $y$  and the transverse momentum  $p_T$ . In this paper, we take

$$|y| < 2.5, \quad p_T > 20 \text{ GeV}. \quad (32)$$

The cuts will also increase the relative correction [25].

In our numerical evaluation, we take a set of independent input parameters which are known from current experiment. The input parameters are  $m_t = 174.2 \text{ GeV}$ ,  $m_b = 4.7 \text{ GeV}$ ,  $G_F = 1.166392 \times 10^{-5} \text{ GeV}^{-2}$ ,  $\sin^2\theta_W = 0.2315$ , and  $\alpha = 1/137.036$  [26]. It is known that the cross section for the  $e^+e^- \rightarrow \gamma\gamma \rightarrow b\bar{b}$  at the tree level is model independent, but the quantum corrections are model dependent. The values of the tree-level cross section are 7.962 pb, 3.040 pb, and 1.668 pb for  $\sqrt{s} = 0.5, 1.0, \text{ and } 1.5 \text{ TeV}$ , respectively.

Since the ETC sector of this model is a one-generation technicolor model. The masses of PGBs are model dependent. In Ref. [17], the masses of  $\pi$  and  $\pi_8$  are taken to be in the range  $60 \text{ GeV} < m_\pi < 200 \text{ GeV}$ ,  $200 \text{ GeV} < m_{\pi_8} < 500 \text{ GeV}$ . In the TOPC sector, the mass of the top pion,  $m_{\pi_t}$ , a reasonable value of the parameter is around 200 GeV. In the following calculation, we would rather take a slightly larger range,  $150 \text{ GeV} < m_{\pi_t} < 450 \text{ GeV}$ , to see its effect, and shall take the masses of  $m_\pi$ , 150 GeV, and  $m_{\pi_8}$ , 246 GeV. The final numerical results are plotted in Figs. 3–5.

Figure 3 shows the relative correction  $\delta\sigma(e^+e^- \rightarrow \gamma\gamma \rightarrow b\bar{b})$  versus  $\varepsilon$  with  $m_\pi = 225 \text{ GeV}$ , and  $\sqrt{s} = 0.5, 1.0, 1.5 \text{ TeV}$ . One can see that (i) the relative corrections are

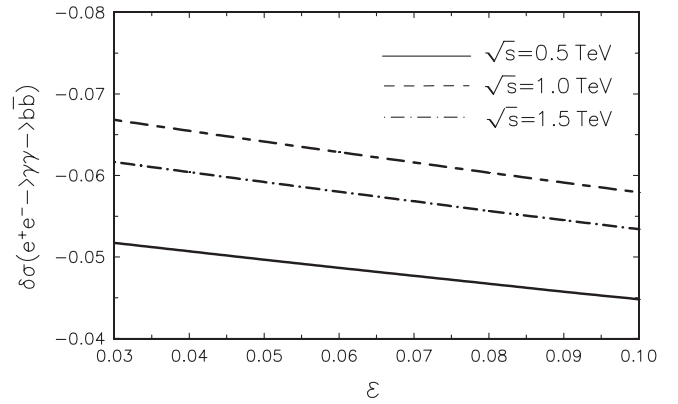


FIG. 3. The relative correction  $\delta\sigma(e^+e^- \rightarrow \gamma\gamma \rightarrow b\bar{b})$  curves as a function of  $\varepsilon$  for  $m_\pi = 150 \text{ GeV}$ ,  $m_{\pi_8} = 246 \text{ GeV}$ , and  $m_{\pi_t} = 246 \text{ GeV}$ .

negative and are between  $-4\%$  and  $-7\%$  in general, (ii) the relative corrections decrease with  $\varepsilon$  slowly, which is natural since the less  $\varepsilon$ , the larger contribution can be afforded by the TOPC sector of this model, (iii) the maximum of the relative corrections is  $-6.8\%$  for  $\varepsilon = 0.03$ , when  $\sqrt{s} = 1.0 \text{ TeV}$ .

Figure 4 presents the plots of relative correction  $\delta\sigma(e^+e^- \rightarrow \gamma\gamma \rightarrow b\bar{b})$  vs  $m_{\pi_t}$  with  $\varepsilon = 0.06$ , and  $\sqrt{s} = 0.5, 1.0, 1.5 \text{ TeV}$ . From this figure, we can see the following: (i) The relative corrections decrease with  $m_{\pi_t}$  sensitively. (ii) The relative corrections at  $\sqrt{s} = 1.0 \text{ TeV}$  are larger than those at  $\sqrt{s} = 0.5 \text{ TeV}$  and  $\sqrt{s} = 1.5 \text{ TeV}$ . (iii) The maximum of the relative corrections can reach  $-7.9\%$  for  $\varepsilon = 0.06$  and  $m_{\pi_t} = 150 \text{ GeV}$  when  $\sqrt{s} = 1.0 \text{ TeV}$ .

Next, we look at the total cross section of the process  $e^+e^- \rightarrow \gamma\gamma \rightarrow b\bar{b}$  arising from PGBs' contribution. We take the case of  $m_\pi = 150 \text{ GeV}$ ,  $m_{\pi_8} = 246 \text{ GeV}$ ,  $m_{\pi_t} = 225 \text{ GeV}$ , and  $\varepsilon = 0.06$  as an example, and plot  $\sigma(s)$  as a function of  $\sqrt{s}$  in Fig. 5. From the graph, we can find that (i) differing from  $\gamma\gamma \rightarrow t\bar{t}$  [3,22], the total cross section of

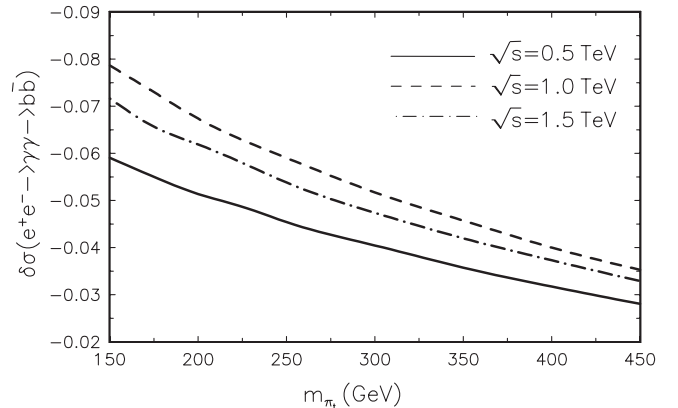


FIG. 4. The relative correction  $\delta\sigma(e^+e^- \rightarrow \gamma\gamma \rightarrow b\bar{b})$  vs  $m_{\pi_t}$ , when  $\varepsilon = 0.06$ ,  $m_\pi = 150 \text{ GeV}$ , and  $m_{\pi_8} = 246 \text{ GeV}$ .

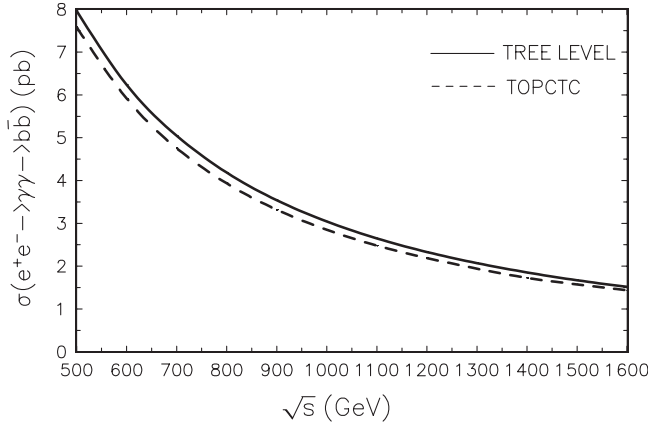


FIG. 5. The total cross sections  $\sigma(s)$  arising from PGBs in the TOPCTC model as a function of  $\sqrt{s}$  with  $\varepsilon = 0.06$ ,  $m_\pi = 150$  GeV,  $m_{\pi_8} = 246$  GeV, and  $m_{\pi_7} = 225$  GeV.

the process  $e^+e^- \rightarrow \gamma\gamma \rightarrow b\bar{b}$  decreases with  $\sqrt{s}$  in the range  $0.5 \sim 1.5$  TeV, (ii) the difference between the TOPCTC model and the tree level is smooth, and has no obvious fluctuation.

For the TOPCMTC model, our calculations show that the contribution from PGBs in the TOPCMTC model is slightly larger than that of the original TOPCTC model and the difference is negligibly small. Therefore the relative corrections  $\delta\sigma(e^+e^- \rightarrow \gamma\gamma \rightarrow b\bar{b})$  and the total cross section  $\sigma(e^+e^- \rightarrow \gamma\gamma \rightarrow b\bar{b})$  in this model are not plotted one by one.

### B. The gauge boson contributions

Now let us consider the contributions from new gauge bosons to the  $\gamma\gamma \rightarrow b\bar{b}$  cross section.

First, for the ETC gauge boson  $Z^*$ , we find that the maximum of the relative corrections  $\delta\sigma_{Z^*}$  is only the order of  $10^{-9} \sim 10^{-10}$  whatever  $\varepsilon$ ,  $\sqrt{s}$ , and  $m_{Z^*}$  taken in the favorable parameter ranges, and therefore can be neglected safely.

Second, for the corrections arising from the color-singlet heavy gauge boson  $Z'$ , in our calculation we assume the mass of the gauge boson  $Z'$  varying from 300 GeV to 1200 GeV to study the effects of  $Z'$  [15]. The numerical results are plotted in Fig. 6. From this figure, we can find that (i) the relative corrections are negative and undulate but not as distinctly as  $m_{Z'}$  increases, (ii) when  $\kappa_1 = 1, 4$ , and 8, the values of relative correction are not more than  $-0.4\%$ ,  $-1.6\%$ , and  $-3.2\%$ , respectively.

Finally, for the new colored gauge bosons  $B$ , our calculations present that the relative correction from these particles is only the order of  $10^{-4} \sim 10^{-5}$  due to their heavy masses, and is negligibly small.

For the TOPCMTC model, our calculations indicate that the contribution from  $Z^*$  in the TOPCMTC model is slightly larger than that of the original TOPCTC model but can be still neglected safely, and the contributions from

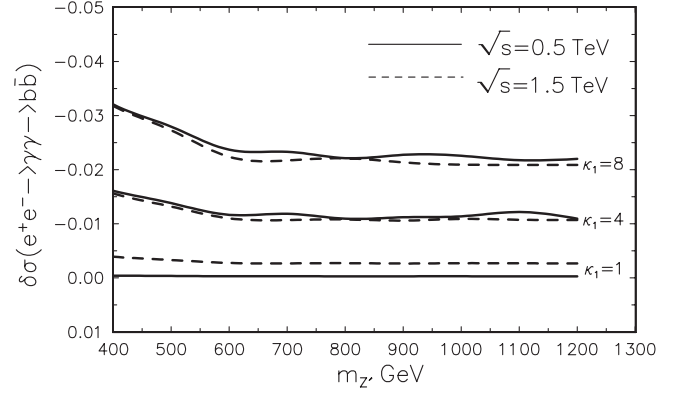


FIG. 6. The relative correction  $\delta\sigma(e^+e^- \rightarrow \gamma\gamma \rightarrow b\bar{b})$  vs  $m_{Z'}$  when  $\kappa_1 = 1, 4$ , and 8.

$Z'$  and  $B$  are the same as those of the original TOPCTC model.

We know the International Linear Collider (ILC) is the important next-generation linear collider. According to the ILC Reference Design Report [27], the ILC is determined to run with  $\sqrt{s} = 500$  GeV and the total luminosity required is  $L = 500 \text{ fb}^{-1}$  with the first four years of operation and  $L = 1000 \text{ fb}^{-1}$  during the first phase of operation with  $\sqrt{s} = 500$  GeV. It means that millions of the bottom pairs per year can be produced, and it can also give obvious changes that the  $-3.2\% \sim -5.9\%$  difference of relative corrections are arising from PGBs contributing in the TOPCTC model when  $\sqrt{s} = 500$  GeV. Furthermore, the new gauge boson  $Z'$  can also afford a less than  $-3.2\%$  relative correction. But this relative correction is less than  $0.1\%$  in the 2HDM and MSSM [5], and for the SM, our calculation shows that this difference from the Higgs boson in the SM is only the order of  $10^{-6}$ , and is negligibly small. Therefore via the process  $\gamma\gamma \rightarrow b\bar{b}$ , the topcolor assisted technicolor models are experimentally distinguishable from the SM, 2HDM, and MSSM, which affords the possibility of testing the topcolor assisted technicolor models.

In conclusion, we have calculated the Yukawa corrections to the process  $\gamma\gamma \rightarrow b\bar{b}$  in the topcolor assisted technicolor models. We find that, for the favorable parameters, the relative corrections from pseudo-Goldstone bosons give out a  $3.2\% \sim 5.9\%$  decrement of the cross section from the tree level when  $\sqrt{s} = 500$  GeV, the contributions from new ETC gauge bosons  $Z^*$  and colored gauge bosons  $B$  are negligibly small, and the relative correction arising from new color-singlet heavy gauge boson  $Z'$  is less than  $-3.2\%$ . Therefore, these corrections are obvious for the International Linear Colliders and are really interesting in testing the standard model and searching for the signs of technicolor.

### ACKNOWLEDGMENTS

This project was supported by the Natural Science Foundation of Henan Educational Committee under

No. 2007140013, the Natural Science Foundation of Henan Province under No. 0611050300, and the National Natural Science Foundation of China under Grant No. 10575029.

and wave function renormalization constants, respectively. Their expressions are listed as

### APPENDIX A: THE FORM FACTORS OF PGBS CONTRIBUTION

The form factors  $f_i^{s(\hat{i})}$  of the PGBs' contribution can be expressed by

$$\begin{aligned} f_1^{s(\hat{i})} &= -2m_b(p_2 \cdot p_4) \left[ \Sigma_S^b(\hat{t}) - \frac{\delta m_b}{m_b} - \delta Z_V^b \right] \\ &\quad - 2m_b(p_2 \cdot p_4) \left[ \Sigma_V^b(\hat{t}) + \delta Z_V^b \right], \\ f_2^{s(\hat{i})} &= 4m_b^2 \left[ \Sigma_S^b(\hat{t}) - \frac{\delta m_b}{m_b} - \delta Z_V^b \right] \\ &\quad + 4(m_b^2 - p_2 \cdot p_4) \left[ \Sigma_V^b(\hat{t}) + \delta Z_V^b \right], \\ f_3^{s(\hat{i})} &= \frac{1}{2} f_2^{s(\hat{i})}, \end{aligned}$$

where  $\Sigma^b$ ,  $\delta m_b$ , and  $\delta Z_V^b$  are the Yukawa contribution part of the unrenormalized self-energy function,  $b$ -quark mass,

$$\Sigma^b(p^2) = \not{p} [\Sigma_V^b(p^2) + \gamma_5 \Sigma_A^b(p^2)] + m_b \Sigma_S^b(p^2).$$

Actually the  $\Sigma_A^b$  does not contribute to the form factor  $f_i^{s(\hat{i})}$  since the term with  $\Sigma_A^b$  includes  $\gamma_5$ :

$$\begin{aligned} \Sigma_V^b(p^2) &= -\frac{\lambda_i^2}{32\pi^2} B_1(p^2, m_t, m_i), \\ \Sigma_A^b(p^2) &= \frac{\lambda_i^2}{32\pi^2} B_1(p^2, m_t, m_i), \\ \Sigma_S^b(p^2) &= 0, \\ \delta m_b &= m_b [\Sigma_V^b(m_b^2) + \Sigma_S^b(m_b^2)], \\ \delta Z_V^b &= -\Sigma_V^b(m_b^2) - 2m_b^2 \frac{\partial}{\partial p^2} [\Sigma_V^b(p^2) + \Sigma_S^b(p^2)]|_{p^2=m_b^2}. \end{aligned}$$

The form factors  $f_i^{v(\hat{i})}$ ,  $f_i^{b(\hat{i})}$ , and  $f_i^{\text{tr}}$  are given by

$$\begin{aligned} f_1^{v(\hat{i})} &= -\frac{\lambda_i^2 Q_t}{16\pi^2} m_b p_2 \cdot p_4 (C_0^2 + C_{11}^2 + C_0^4 + C_{11}^4), \\ f_2^{v(\hat{i})} &= \frac{\lambda_i^2}{8\pi^2} p_2 \cdot p_4 [(C_{12}^3 + C_{23}^3) + Q_t (C_{12}^4 + C_{23}^4)], \\ f_3^{v(\hat{i})} &= \frac{\lambda_i^2}{8\pi^2} [-m_b^2 (C_{11}^1 + C_{21}^1) + p_2 \cdot p_4 (C_{12}^1 + C_{23}^1) + (-C_{24}^1 + C_{24}^3)] \\ &\quad + \frac{\lambda_i^2 Q_t}{16\pi^2} [(m_t^2 + m_b^2)(C_0^2 + C_0^4) + 2m_b^2 C_{11}^2 + 2p_2 \cdot p_4 (C_{12}^4 + C_{23}^4) + m_b^2 (C_{21}^2 - C_{21}^4) - 2(C_{24}^2 + C_{24}^4)] - 4Q_t \delta Z_V^b, \\ f_4^{v(\hat{i})} &= -\frac{\lambda_i^2}{8\pi^2} m_b [(C_{11}^3 + C_{21}^3) + Q_t (C_{11}^4 + C_{21}^4)], \\ f_5^{v(\hat{i})} &= \frac{\lambda_i^2}{16\pi^2} [-C_{24}^1 + C_{24}^3] + \frac{\lambda_i^2 Q_t}{32\pi^2} [(m_t^2 + m_b^2)(C_0^2 + C_0^4) + 2p_2 \cdot p_4 (C_{12}^2 + C_{23}^2 + C_{12}^4 + C_{23}^4) - m_b^2 (C_{21}^2 + C_{21}^4) \\ &\quad - 2(C_{24}^2 + C_{24}^4)] - 2Q_t \delta Z_V^b, \\ f_6^{v(\hat{i})} &= \frac{1}{2} f_4^{v(\hat{i})}, \\ f_7^{v(\hat{i})} &= \frac{\lambda_i^2}{16\pi^2} m_b [(C_{11}^1 + C_{21}^1) - Q_t (C_{11}^2 + C_{21}^2)]. \end{aligned}$$

$$\begin{aligned} f_1^{b(\hat{i})} &= \frac{1}{2} \lambda_i^2 Q_t^2 m_b [m_t^2 (D_0^1 + D_{11}^1) + m_b^2 (-D_0^1 - 2D_{11}^1 + D_{12}^1 - D_{13}^1 - 2D_{21}^1 - D_{23}^1 + 2D_{24}^1 - 2D_{25}^1 - D_{31}^1 + D_{34}^1 - D_{35}^1) \\ &\quad + \hat{s}(D_{25}^1 - D_{26}^1 + D_{35}^1 - D_{310}^1) + \hat{t}(-D_{11}^1 - D_{12}^1 + D_{13}^1 - D_{21}^1 - 2D_{24}^1 + 2D_{25}^1 - D_{34}^1 - D_{35}^1) - 4(D_{27}^1 + D_{311}^1)] \\ &\quad + \lambda_i^2 Q_t m_b (D_{27}^2 + D_{311}^2 - D_{312}^2 + D_{313}^2) - \lambda_i^2 m_b D_{311}^3, \\ f_2^{b(\hat{i})} &= \lambda_i^2 Q_t^2 m_b (D_{27}^1 + D_{311}^1) + \lambda_i^2 Q_t m_b (D_{27}^2 + D_{311}^2 - D_{312}^2 + D_{313}^2) - \lambda_i^2 m_b D_{311}^3, \end{aligned}$$

$$\begin{aligned}
f_3^{b(\hat{\eta})} &= \lambda_i^2 Q_i^2 [m_i^2 (-D_{12}^1 + D_{13}^1) + m_b^2 (D_{12}^1 - D_{13}^1 - D_{22}^1 + 3D_{23}^1 + 2D_{24}^1 - D_{25}^1 - D_{26}^1 + D_{34}^1 - D_{35}^1 - D_{36}^1 - D_{38}^1) \\
&\quad + \hat{s}(D_{37}^1 + D_{38}^1 - D_{39}^1 - D_{310}^1) + \hat{t}(D_{22}^1 - 3D_{23}^1 - D_{25}^1 + D_{26}^1 + D_{36}^1 + D_{38}^1) + 2(D_{27}^1 + 2D_{312}^1 - 3D_{313}^1)] \\
&\quad + \lambda_i^2 Q_i [m_i^2 (-D_{11}^2 + D_{12}^2) + m_b^2 (D_{11}^2 - D_{12}^2 + D_{21}^2 - 3D_{22}^2 - D_{24}^2 + 2D_{25}^2 - 2D_{26}^2 - D_{32}^2 - D_{34}^2 + 2D_{35}^2 + 4D_{36}^2 \\
&\quad + 3D_{37}^2 + 2D_{38}^2 - 5D_{310}^2) + \hat{s}(2D_{22}^2 - D_{36}^2 - D_{37}^2 - D_{38}^2 - D_{39}^2 + D_{310}^2) + \hat{t}(D_{21}^2 + D_{22}^2 - 2D_{24}^2 + D_{31}^2 - 2D_{34}^2 \\
&\quad - D_{36}^2 - D_{37}^2 - D_{38}^2 - D_{39}^2 + D_{310}^2) + 2(D_{27}^2 + 2D_{311}^2 - 2D_{312}^2)] - 2\lambda_i^2 (D_{27}^3 - D_{312}^3), \\
f_4^{b(\hat{\eta})} &= \lambda_i^2 Q_i^2 [-m_i^2 D_{13}^1 + m_b^2 (-D_{13}^1 + D_{23}^1 - D_{25}^1 + D_{35}^1 + D_{38}^1 - D_{310}^1) + \hat{s}(-D_{38}^1 + D_{39}^1) + \hat{t}(-D_{23}^1 + D_{25}^1 - D_{38}^1 \\
&\quad + D_{310}^1) + 4D_{311}^1] + 2\lambda_i^2 Q_i (D_{312}^2 - D_{313}^2) + 2\lambda_i^2 D_{313}^3, \\
f_5^{b(\hat{\eta})} &= \lambda_i^2 Q_i^2 [m_i^2 (D_{11}^1 - D_{12}^1) + m_b^2 (-D_{11}^1 + D_{12}^1 - 2D_{21}^1 - D_{22}^1 + 3D_{24}^1 - 2D_{26}^1 - D_{31}^1 + 2D_{34}^1 - D_{35}^1 - D_{36}^1 - 2D_{38}^1 \\
&\quad - D_{310}^1) + \hat{s}(D_{35}^1 + D_{37}^1 - 2D_{310}^1) + \hat{t}(D_{22}^1 - D_{24}^1 + 2D_{26}^1 - D_{34}^1 + D_{35}^1 + D_{36}^1 + D_{310}^1) - 4(D_{311}^1 + D_{312}^1)] \\
&\quad + \lambda_i^2 Q_i [m_i^2 D_{13}^2 + m_b^2 (-2D_{23}^2 - D_{25}^2 + D_{26}^2 - 2D_{33}^2 - D_{37}^2 - 2D_{38}^2 + 3D_{39}^2 + D_{310}^2) + \hat{s}(D_{33}^2 - D_{39}^2) + \hat{t}(-D_{25}^2 \\
&\quad + D_{26}^2 + D_{33}^2 - D_{35}^2 - D_{39}^2 + D_{310}^2) - 4D_{313}^2] - 2\lambda_i^2 (2D_{27}^3 + D_{311}^3 - D_{312}^3), \\
f_6^{b(\hat{\eta})} &= \lambda_i^2 Q_i^2 [m_i^2 D_0^1 + m_b^2 (D_0^1 + 2D_{11}^1 - 2D_{13}^1 + D_{21}^1 - 3D_{25}^1 + D_{26}^1 + 2D_{38}^1) + \hat{s}(D_{25}^1 - D_{26}^1) + \hat{t}(D_{25}^1 - D_{26}^1) + 2(D_{311}^1 \\
&\quad - D_{313}^1)] + 2\lambda_i^2 Q_i (D_{27}^2 + D_{311}^2) - 2\lambda_i^2 (D_{27}^3 + D_{311}^3 - D_{313}^3), \\
f_7^{b(\hat{\eta})} &= 2\lambda_i^2 Q_i^2 m_b (D_{26}^1 + D_{310}^1) + 2\lambda_i^2 Q_i m_b (D_{22}^2 - D_{24}^2 + D_{25}^2 - D_{26}^2 - D_{32}^2 - D_{34}^2 + D_{35}^2 + 2D_{36}^2 + 2D_{37}^2 + D_{38}^2 - D_{39}^2 \\
&\quad - 3D_{310}^2) + 2\lambda_i^2 m_b (D_{25}^3 - D_{310}^3), \\
f_8^{b(\hat{\eta})} &= 2\lambda_i^2 Q_i^2 m_b (-D_{25}^1 + D_{26}^1 - D_{35}^1 + D_{310}^1) + 2\lambda_i^2 Q_i m_b (-D_{23}^2 + D_{26}^2 - D_{33}^2 - D_{37}^2 - D_{38}^2 + 2D_{39}^2 + D_{310}^2) \\
&\quad + 2\lambda_i^2 m_b (2D_{25}^3 + D_{35}^3 - D_{310}^3), \\
f_9^{b(\hat{\eta})} &= 2\lambda_i^2 Q_i^2 m_b (-D_{12}^1 - 2D_{24}^1 + D_{26}^1 - D_{34}^1 + D_{310}^1) + 2\lambda_i^2 Q_i m_b (-D_{11}^2 + D_{12}^2 - 2D_{21}^2 - D_{22}^2 + 3D_{24}^2 - D_{25}^2 + D_{26}^2 \\
&\quad - D_{31}^2 + 2D_{34}^2 - D_{35}^2 - D_{36}^2 + D_{310}^2) + 2\lambda_i^2 m_b (-D_{11}^3 - D_{21}^3 + D_{24}^3 + D_{25}^3 + D_{34}^3 - D_{310}^3), \\
f_{10}^{b(\hat{\eta})} &= 2\lambda_i^2 Q_i^2 m_b (D_{11}^1 - D_{12}^1 + 2D_{21}^1 - 2D_{24}^1 - D_{25}^1 + D_{26}^1 + D_{31}^1 - D_{34}^1 - D_{35}^1 + D_{310}^1) + 2\lambda_i^2 Q_i m_b (D_{23}^2 + 2D_{25}^2 \\
&\quad - D_{26}^2 + D_{35}^2 + D_{38}^2 - D_{310}^2) + 2\lambda_i^2 m_b (-2D_{11}^3 - 3D_{21}^3 + D_{24}^3 + 2D_{25}^3 - D_{31}^3 + D_{34}^3 + D_{35}^3 - D_{310}^3), \\
f_{11}^{b(\hat{\eta})} &= \frac{1}{2} \lambda_i^2 Q_i^2 [m_i^2 (D_0^1 - D_{12}^1 + 2D_{13}^1) + m_b^2 (D_0^1 + D_{12}^1 - D_{13}^1 - D_{21}^1 - D_{22}^1 - D_{23}^1 + 4D_{24}^1 - 2D_{25}^1 + D_{31}^1 - D_{35}^1 - D_{36}^1 \\
&\quad - D_{38}^1 - D_{310}^1) + \hat{s}(D_{25}^1 - D_{26}^1 + D_{37}^1 + D_{38}^1 + D_{39}^1 - D_{310}^1) + \hat{t}(D_{22}^1 + D_{23}^1 + D_{36}^1 + D_{38}^1 - D_{310}^1) + 2(2D_{312}^1 \\
&\quad - D_{313}^1)] - \lambda_i^2 Q_i (D_{311}^2 - D_{313}^2) + \lambda_i^2 (D_{312}^3 - D_{313}^3), \\
f_{12}^{b(\hat{\eta})} &= -\lambda_i^2 Q_i^2 (D_{27}^1 + D_{313}^1) - \lambda_i^2 Q_i (D_{27}^2 + D_{311}^2 - D_{313}^2) + \lambda_i^2 (D_{312}^3 - D_{313}^3), \\
f_{13}^{b(\hat{\eta})} &= \lambda_i^2 Q_i^2 m_b (-D_{12}^1 + D_{22}^1 - D_{24}^1 - 2D_{25}^1 + 2D_{26}^1 + 2D_{310}^1) + \lambda_i^2 Q_i m_b (-D_{11}^2 + D_{12}^2 - D_{21}^2 - D_{22}^2 + 2D_{24}^2 - D_{25}^2 \\
&\quad + D_{26}^2), \\
f_{14}^{b(\hat{\eta})} &= \lambda_i^2 Q_i^2 m_b (D_{23}^1 + D_{25}^1), \\
f_{15}^{b(\hat{\eta})} &= \lambda_i^2 Q_i^2 m_b (D_{11}^1 - D_{12}^1 + D_{21}^1 + D_{22}^1 - D_{24}^1 + 2D_{26}^1 + 2D_{310}^1) + \lambda_i^2 Q_i m_b (D_{13}^2 + D_{25}^2 - D_{26}^2),
\end{aligned}$$

$$\begin{aligned}
f_{16}^{b(\hat{t})} &= -\lambda_i^2 Q_i^2 m_b (D_{11}^1 - D_{13}^1 + D_{21}^1 - D_{25}^1), \\
f_{17}^{b(\hat{t})} &= 2\lambda_i^2 Q_i^2 (D_{23}^1 - D_{26}^1 - D_{37}^1 + D_{39}^1) + 2\lambda_i^2 Q_i (-D_{22}^2 + D_{24}^2 - D_{25}^2 + D_{26}^2 + D_{34}^2 - D_{35}^2 - D_{36}^2 + D_{37}^2 + D_{38}^2 - D_{39}^2) \\
&\quad + 2\lambda_i^2 (D_{23}^3 - D_{26}^3 + D_{37}^3 - D_{39}^3), \\
f_{18}^{b(\hat{t})} &= 2\lambda_i^2 Q_i^2 (D_{25}^1 - D_{26}^1 - D_{37}^1 - D_{38}^1 + D_{39}^1 + D_{310}^1) + 2\lambda_i^2 Q_i (D_{23}^2 - D_{26}^2 - D_{33}^2 + D_{38}^2 + D_{39}^2 - D_{310}^2) + 2\lambda_i^2 (2D_{23}^3 \\
&\quad - 2D_{26}^3 + D_{37}^3 + D_{38}^3 - D_{39}^3 - D_{310}^3), \\
f_{19}^{b(\hat{t})} &= 2\lambda_i^2 Q_i^2 (D_{22}^1 + D_{23}^1 - D_{25}^1 + D_{26}^1 + D_{36}^1 - D_{37}^1 + D_{39}^1 + D_{310}^1) + 2\lambda_i^2 Q_i (D_{21}^2 - D_{25}^2 + D_{26}^2 + D_{31}^2 - D_{34}^2 - D_{35}^2 \\
&\quad + D_{310}^2) + 2\lambda_i^2 (D_{12}^3 - D_{13}^3 - D_{22}^3 + D_{23}^3 + D_{24}^3 - D_{25}^3 - D_{36}^3 + D_{37}^3 - D_{39}^3 + D_{310}^3), \\
f_{20}^{b(\hat{t})} &= 2\lambda_i^2 Q_i^2 (D_{22}^1 - D_{24}^1 + D_{25}^1 + D_{26}^1 - D_{34}^1 + D_{35}^1 + D_{36}^1 - D_{37}^1 - D_{38}^1 + D_{39}^1 + 2D_{310}^1) + 2\lambda_i^2 Q_i (D_{23}^2 - D_{24}^2 - D_{25}^2 \\
&\quad - D_{25}^2 + D_{38}^2) + 2\lambda_i^2 (2D_{12}^3 - 2D_{13}^3 - D_{22}^3 + 2D_{23}^3 + 3D_{24}^3 - 3D_{25}^3 - D_{26}^3 + D_{34}^3 - D_{35}^3 - D_{36}^3 + D_{37}^3 + D_{38}^3 \\
&\quad - D_{39}^3), \\
f_1^{\text{tr}} &= -\frac{1}{2} \lambda_i^2 m_b C_{11}^5,
\end{aligned}$$

where

$$\begin{aligned}
C^1 &= C(-p_2, p_4, m_t, m_b, m_i), & C^2 &= C(p_2, -p_4, m_t, m_t, m_t), & C^3 &= C(p_1, -p_3, m_t, m_b, m_i), \\
C^4 &= C(-p_1, p_3, m_t, m_t, m_t), & C^5 &= C(-p_2, p_1 + p_2, m_t, m_b, m_i), & D^1 &= D(p_2, -p_4, -p_3, m_t, m_t, m_t, m_t), \\
D^2 &= D(-p_1 + p_3, p_1, -p_1 + p_4, m_t, m_t, m_t, m_t), & D^3 &= D(-p_2, p_4, p_3, m_t, m_t, m_t, m_t),
\end{aligned}$$

and

$$\begin{aligned}
\hat{s} &= (p_1 + p_2)^2, & \hat{t} &= (p_4 - p_2)^2, \\
\hat{u} &= (p_4 - p_1)^2.
\end{aligned}$$

For  $i = \pi$ ,

$$\lambda_\pi = \frac{c_t \varepsilon m_t}{f_\pi},$$

for  $i = \pi_8$ ,

$$\lambda_{\pi_8} = \frac{\varepsilon m_t \lambda^a}{f_\pi},$$

and for  $i = \pi_t$ ,

$$\lambda_t = \frac{(1 - \varepsilon) m_t}{f_{\pi_t}}.$$

## APPENDIX B: THE FORM FACTORS ARISING FROM NEW GAUGE BOSONS

The form factors  $f_i^{s(\hat{t})}$  from new gauge bosons ( $Z^*$ ,  $Z'$ , and  $B$ ) can be written as

$$\begin{aligned}
f_1^{s(\hat{t})} &= -2m_b(p_2 \cdot p_4) \left[ \Sigma_S^b(\hat{t}) - \frac{\delta m_b}{m_b} - \delta Z_V^b \right] \\
&\quad - 2m_b(p_2 \cdot p_4) [\Sigma_V^b(\hat{t}) + \delta Z_V^b], \\
f_2^{s(\hat{t})} &= 4m_b^2 \left[ \Sigma_S^b(\hat{t}) - \frac{\delta m_b}{m_b} - \delta Z_V^b \right] \\
&\quad + 4(m_b^2 - p_2 \cdot p_4) [\Sigma_V^b(\hat{t}) + \delta Z_V^b], \\
f_3^{s(\hat{t})} &= \frac{1}{2} f_2^{s(\hat{t})},
\end{aligned}$$

where

$$\begin{aligned}
\Sigma_V^b(p^2) &= -\frac{1}{16\pi^2} (\lambda_1^2 + \lambda_2^2) B_1(p^2, m_b, m_i), \\
\Sigma_S^b(p^2) &= -\frac{1}{4\pi^2} \lambda_1 \lambda_2 B_0(p^2, m_b, m_i), \\
\delta m_b &= m_b [\Sigma_V^b(m_b^2) + \Sigma_S^b(m_b^2)],
\end{aligned}$$

and

$$\delta Z_V^b = -\Sigma_V^b(m_b^2) - 2m_b^2 \frac{\partial}{\partial p^2} [\Sigma_V^b(p^2) + \Sigma_S^b(p^2)] \Big|_{p^2=m_b^2}.$$

The form factors  $f_i^{v(\hat{t})}$ , and  $f_i^{b(\hat{t})}$  are given by

$$f_1^{v(\hat{i})} = \frac{1}{8\pi^2} m_b p_2 \cdot p_4 Q_b (\lambda_1^2 + \lambda_2^2) (C_0^1 + C_{11}^1 + C_0^2 + C_{11}^2),$$

$$f_2^{v(\hat{i})} = \frac{1}{4\pi^2} p_2 \cdot p_4 Q_b (\lambda_1^2 + \lambda_2^2) (C_0^2 + C_{11}^2 + C_{12}^2 + C_{23}^2),$$

$$f_3^{v(\hat{i})} = \frac{1}{8\pi^2} Q_b [2m_b^2 (\lambda_1^2 + \lambda_2^2) (C_0^1 + C_{11}^1 - C_0^2 - 2C_{11}^2) + 2p_2 \cdot p_4 (\lambda_1^2 + \lambda_2^2) (C_0^2 + C_{11}^2 + C_{12}^2 + C_{23}^2) + m_b^2 (\lambda_1^2 + \lambda_2^2) \times (C_{21}^1 - C_{21}^2) - 8m_b^2 \lambda_1 \lambda_2 (C_0^1 + C_{11}^1) - 2(\lambda_1^2 + \lambda_2^2) (C_{24}^1 + C_{24}^2)] - 4Q_b \delta Z_V^b,$$

$$f_4^{v(\hat{i})} = \frac{1}{4\pi^2} m_b Q_b [4\lambda_1 \lambda_2 (C_0^2 + C_{11}^2) - (\lambda_1^2 + \lambda_2^2) (2C_0^2 + 3C_{11}^2 + C_{21}^2)],$$

$$f_5^{v(\hat{i})} = \frac{1}{16\pi^2} Q_b [-2m_b^2 (\lambda_1^2 + \lambda_2^2) (C_0^1 + 2C_{11}^1 + C_0^2 + 2C_{11}^2) - m_b^2 (\lambda_1^2 + \lambda_2^2) (C_{21}^1 + C_{21}^2) + 2p_2 \cdot p_4 (\lambda_1^2 + \lambda_2^2) (C_0^1 + C_{11}^1 + C_{12}^1 + C_{23}^1 + C_0^2 + C_{11}^2 + C_{12}^2 + C_{23}^2) - 2(\lambda_1^2 + \lambda_2^2) (C_{24}^1 + C_{24}^2)] - 2Q_b \delta Z_V^b,$$

$$f_6^{v(\hat{i})} = \frac{1}{2} f_4^{v(\hat{i})}, \quad f_7^{v(\hat{i})} = \frac{1}{8\pi^2} m_b Q_b [4\lambda_1 \lambda_2 (C_0^1 + C_{11}^1) - (\lambda_1^2 + \lambda_2^2) (2C_0^1 + 3C_{11}^1 + C_{21}^1)].$$

$$f_1^{b(\hat{i})} = Q_b^2 [m_b^3 (\lambda_1^2 + \lambda_2^2) (2D_0 + 2D_{11} + D_{12} - 2D_{13} + 2D_{23} - D_{25}) - m_b \hat{s} (\lambda_1^2 + \lambda_2^2) (D_0 + D_{11} - D_{13} + D_{23}) - m_b \hat{t} (\lambda_1^2 + \lambda_2^2) (2D_0 + 2D_{11} + D_{12} - 2D_{13} + 2D_{23} - D_{25}) - 2m_b (\lambda_1^2 + \lambda_2^2) (D_{27} - D_{313}) + 2m_b^3 \lambda_1 \lambda_2 (2D_{11} - D_{12} + D_{25}) - 2m_b \hat{s} \lambda_1 \lambda_2 (D_0 + D_{25} - D_{26}) + 2m_b \hat{t} \lambda_1 \lambda_2 (2D_0 + D_{12} + D_{21} + D_{24} - D_{25})],$$

$$f_2^{b(\hat{i})} = Q_b^2 [-m_b^3 (\lambda_1^2 + \lambda_2^2) (D_{11} - D_{12} + D_{13} + 2D_{21} - 2D_{23} - 2D_{24} + 5D_{25} + D_{31} + D_{34} + D_{35} - 2D_{38} - 2D_{39} + 2D_{310}) - m_b \hat{s} (\lambda_1^2 + \lambda_2^2) (2D_{23} - 3D_{25} + D_{26} - D_{35} + 2D_{38} + 2D_{39} - D_{310}) - m_b \hat{t} (\lambda_1^2 + \lambda_2^2) (D_{11} + D_{12} - D_{13} + D_{21} + 2D_{23} + 2D_{24} - 4D_{25} - D_{34} - D_{35} + 2D_{38} + 2D_{39} - 2D_{310}) - 4m_b (\lambda_1^2 + \lambda_2^2) (D_{27} + D_{311}) + 2m_b^2 \lambda_1 \lambda_2 (2D_0 + D_{11} - D_{12} - 3D_{13} + D_{21} - D_{24} + D_{25}) + 2m_b \hat{s} \lambda_1 \lambda_2 (2D_{13} - D_{25} + D_{26}) + 2m_b \hat{t} \lambda_1 \lambda_2 (D_{11} + D_{12} - D_{13} + D_{24} - D_{25})],$$

$$f_3^{b(\hat{i})} = Q_b^2 [2m_b^2 (\lambda_1^2 + \lambda_2^2) (2D_{11} + 2D_{21} - 3D_{23} - D_{24} + 3D_{25} + D_{35} - D_{38} - D_{310}) - 2\hat{s} (\lambda_1^2 + \lambda_2^2) (D_{13} - D_{23} + D_{24} + 2D_{25} - D_{26} - D_{39}) + 2\hat{t} (\lambda_1^2 + \lambda_2^2) (2D_{12} - 2D_{13} + D_{24} - D_{25} + D_{38} + D_{310}) - 4(\lambda_1^2 + \lambda_2^2) (D_{27} + D_{312} - 3D_{313})],$$

$$f_4^{b(\hat{i})} = Q_b^2 [-2m_b^2 (\lambda_1^2 + \lambda_2^2) (2D_{11} - D_{12} + D_{21} - D_{23} - D_{24} - 3D_{25} + D_{26}) - 4\hat{t} (\lambda_1^2 + \lambda_2^2) (D_{12} - D_{13} + D_{24} - D_{26}) - 4(\lambda_1^2 + \lambda_2^2) (D_{27} + D_{313}) + 4m_b^2 \lambda_1 \lambda_2 (2D_0 + D_{13})],$$

$$f_5^{b(\hat{i})} = Q_b^2 [-2m_b^2 (\lambda_1^2 + \lambda_2^2) (2D_0 + D_{12} - D_{13} - 2D_{21} + D_{22} + D_{24} - 2D_{25} - D_{26}) + 2\hat{t} (\lambda_1^2 + \lambda_2^2) (D_{12} - D_{13} - D_{21} + D_{22} + D_{24} - D_{26}) + 4(\lambda_1^2 + \lambda_2^2) (D_{27} + D_{311} - D_{312})],$$

$$f_6^{b(\hat{i})} = Q_b^2 [-2m_b^2 (\lambda_1^2 + \lambda_2^2) (2D_0 + 6D_{11} - 2D_{12} - 5D_{21} - D_{23} - 3D_{24} - 2D_{25} + 2D_{26} + D_{31} - D_{34} - D_{38} + D_{310}) + 2\hat{s} (\lambda_1^2 + \lambda_2^2) (D_0 + 2D_{11} - D_{12} + D_{21} - D_{24} + D_{35} - D_{38} + D_{39} - D_{310}) - 2\hat{t} (\lambda_1^2 + \lambda_2^2) (2D_{12} - 2D_{13} + D_{23} + 3D_{24} - 2D_{25} - 2D_{26} + D_{34} - D_{35} + D_{38} - D_{310}) - 8(\lambda_1^2 + \lambda_2^2) (D_{27} + D_{311} - D_{313}) + 4m_b^2 \lambda_1 \lambda_2 (2D_0 + D_{13})],$$

$$f_7^{b(\hat{i})} = 4m_b Q_b^2 [(\lambda_1^2 + \lambda_2^2) (2D_{13} + 2D_{25} + D_{26} + D_{310}) - 2\lambda_1 \lambda_2 (D_{13} + 2D_{26})],$$

$$f_8^{b(\hat{i})} = 4m_b Q_b^2 [(\lambda_1^2 + \lambda_2^2) (D_{26} - D_{35} + D_{310}) + 4\lambda_1 \lambda_2 (D_{25} - D_{26})],$$

$$\begin{aligned}
f_9^{b(\hat{i})} &= 4m_b Q_b^2 [-(\lambda_1^2 + \lambda_2^2)(D_0 + 3D_{11} + D_{12} - 2D_{13} + 2D_{21} + 2D_{24} - 2D_{25} - D_{26} + D_{34} - D_{310}) + 2\lambda_1 \lambda_2 (2D_0 \\
&\quad + 2D_{11} + 2D_{12} - D_{13} + 2D_{24} - 2D_{26})], \\
f_{10}^{b(\hat{i})} &= 4m_b Q_b^2 [(\lambda_1^2 + \lambda_2^2)(D_0 + 2D_{11} - D_{12} + 2D_{21} - 2D_{24} - D_{25} + D_{26} + D_{31} - D_{34} - D_{35} + D_{310}) - 2\lambda_1 \lambda_2 (D_0 \\
&\quad + 2D_{11} - 2D_{12} + 2D_{21} - 2D_{24} - 2D_{25} + 2D_{26})], \\
f_{11}^{b(\hat{i})} &= Q_b^2 [-4m_b^2 (\lambda_1^2 + \lambda_2^2)(D_0 + D_{11} + D_{12}) + \hat{s}(\lambda_1^2 + \lambda_2^2)(D_0 + D_{11}) - 2(\lambda_1^2 + \lambda_2^2)(D_{27} + D_{312} - D_{313}) \\
&\quad + 2m_b^2 \lambda_1 \lambda_2 D_{13}], \\
f_{12}^{b(\hat{i})} &= Q_b^2 [m_b^2 (\lambda_1^2 + \lambda_2^2)(2D_0 - D_{13} - D_{21} - D_{22} - D_{23} + 2D_{24} - 2D_{25} + 2D_{26} + D_{34} - D_{35} - D_{36} - D_{38} + 2D_{310}) \\
&\quad + \hat{s}(\lambda_1^2 + \lambda_2^2)(D_{25} - D_{26} + D_{37} + D_{38} - D_{39} - D_{310}) + \hat{i}(\lambda_1^2 + \lambda_2^2)(D_{22} + D_{23} - 2D_{26} + D_{36} + D_{38} - 2D_{310}) \\
&\quad + 4(\lambda_1^2 + \lambda_2^2)(D_{312} - D_{313}) - 2m_b^2 \lambda_1 \lambda_2 (2D_0 + 3D_{13})], \\
f_{13}^{b(\hat{i})} &= 2m_b Q_b^2 [(\lambda_1^2 + \lambda_2^2)(D_0 + D_{11} - D_{12} - D_{24}) + 2\lambda_1 \lambda_2 (D_0 + D_{13})], \\
f_{14}^{b(\hat{i})} &= 2m_b Q_b^2 [(\lambda_1^2 + \lambda_2^2)(D_0 + D_{11} - D_{13} - D_{25}) - 2\lambda_1 \lambda_2 (D_0 + D_{13})], \\
f_{15}^{b(\hat{i})} &= 2m_b Q_b^2 [(\lambda_1^2 + \lambda_2^2)(D_0 + D_{12} - D_{21}) - 2\lambda_1 \lambda_2 D_0], \\
f_{16}^{b(\hat{i})} &= 2m_b Q_b^2 [-(\lambda_1^2 + \lambda_2^2)(D_0 + D_{13} - D_{21} + D_{25}) + 2\lambda_1 \lambda_2 D_0], \\
f_{17}^{b(\hat{i})} &= 4Q_b^2 (\lambda_1^2 + \lambda_2^2)(D_{23} - D_{26} - D_{37} + D_{39}), \quad f_{18}^{b(\hat{i})} = -4Q_b^2 (\lambda_1^2 + \lambda_2^2)(D_{25} - D_{26} + D_{37} + D_{38} - D_{39} - D_{310}), \\
f_{19}^{b(\hat{i})} &= 4Q_b^2 (\lambda_1^2 + \lambda_2^2)(2D_{12} - 2D_{13} + D_{22} + D_{23} + 2D_{24} - D_{25} - 3D_{26} + D_{36} - D_{37} + D_{39} - D_{310}), \\
f_{20}^{b(\hat{i})} &= 4Q_b^2 (\lambda_1^2 + \lambda_2^2)(D_{22} - D_{24} - D_{34} + D_{35} + D_{36} - D_{37} - D_{38} + D_{39}),
\end{aligned}$$

with

$$C^1 = C(p_2, -p_4, m_i, m_b, m_b), \quad C^2 = C(-p_1, p_3, m_i, m_b, m_b), \quad D = D(p_2, -p_4, -p_3, m_i, m_b, m_b, m_b).$$

For  $i = Z^*$ ,

$$\lambda_1 = -\frac{\varepsilon m_t}{16\pi f_\pi} \frac{e}{s_W c_W} \left[ \frac{N_C}{N_{TC} + 1} \xi_t (\xi_t^{-1} + \xi_b) - \xi_t^2 \right], \quad \lambda_2 = 0,$$

for  $i = Z'$ ,

$$\lambda_1 = \frac{1}{6} g_1 \cot\theta', \quad \lambda_2 = -\frac{1}{3} g_1 \cot\theta',$$

and for  $i = B$ ,

$$\lambda_1 = \lambda_2 = \frac{1}{2} g_3 \cot\theta \lambda^a.$$

- 
- [1] S. J. Brodsky and P. M. Zerwas, Nucl. Instrum. Methods Phys. Res., Sect. A **355**, 19 (1995).  
[2] I. F. Ginzburg, G. L. Kotkin, V. G. Serbo, and V. I. Telnov, Zh. Eksp. Teor. Fiz. **34**, 514 (1981); Nucl. Instrum. Methods. **205**, 47 (1983).  
[3] F. Halzen, C. S. Kim, and M. L. Stong, Phys. Lett. B **274**, 489 (1992).  
[4] O. J. P. Eboli, M. C. Gonzalez-Garcia, F. Halzen, and S. F. Novaes, Phys. Rev. D **47**, 1889 (1993).  
[5] L. Han, C. G. Hu, C. S. Li, and W. G. Ma, Phys. Rev. D **54**, 2363 (1996).  
[6] S. Weinberg, Phys. Rev. D **19**, 1277 (1979); L. Susskind, *ibid.* **20**, 2619 (1979).  
[7] S. Dimopoulos and L. Susskind, Nucl. Phys. **B155**, 237

- (1979); E. Eichten and K. Lane, Phys. Lett. B **90**, 125 (1980).
- [8] B. Holdom, Phys. Rev. D **24**, 1441 (1981); Phys. Lett. B **150**, 301 (1985); T. Appelquist, D. Karabali, and L. C. R. Wijewardhana, Phys. Rev. Lett. **57**, 957 (1986); T. Appelquist and L. C. R. Wijewardhana, Phys. Rev. D **36**, 568 (1987); K. Yamawaki, M. Bando, and K. Matumoyo, Phys. Rev. Lett. **56**, 1335 (1986); T. Akiba and T. Yanagida, Phys. Lett. B **169**, 432 (1986).
- [9] K. Lane and E. Eichten, Phys. Lett. B **222**, 274 (1989); K. Lane and M. V. Ramana, Phys. Rev. D **44**, 2678 (1991).
- [10] R. S. Chivukula, S. B. Selipsky, and E. H. Simmons, Phys. Rev. Lett. **69**, 575 (1992); R. S. Chivukula, E. H. Simmons, and J. Terning, Phys. Lett. B **331**, 383 (1994).
- [11] C. T. Hill, Phys. Lett. B **345**, 483 (1995); C. T. Hill *et al.*, Phys. Rep. **381**, 235 (2003).
- [12] K. Lane and E. Eichten, Phys. Lett. B **352**, 382 (1995); K. Lane, Phys. Rev. D **54**, 2204 (1996); Phys. Lett. B **433**, 96 (1998).
- [13] C. T. Hill, Phys. Lett. B **266**, 419 (1991); S. P. Martin, Phys. Rev. D **45**, 4283 (1992); **46**, 2197 (1992); Nucl. Phys. **B398**, 359 (1993); M. Lindner and D. Ross, Nucl. Phys. **B370**, 30 (1992); R. Bönisch, Phys. Lett. B **268**, 394 (1991).
- [14] G. R. Lu, Z. H. Xiong, and Y. G. Cao, Nucl. Phys. **B487**, 43 (1997); Z. J. Xiao, W. J. Li, L. B. Guo, and G. R. Lu, Eur. Phys. J. C **18**, 681 (2001); Jinshu Huang and Qunna Pan, Commun. Theor. Phys. **42**, 573 (2004); G. R. Lu, F. R. Yin, X. L. Wang, and L. D. Wan, Phys. Rev. D **68**, 015002 (2003); X. L. Wang, Y. L. Yang, and B. Z. Li, *ibid.* **69**, 055002 (2004); C. X. Yue, H. J. Zong, and W. Wang, J. Phys. G **29**, 2145 (2003); C. X. Yue, L. H. Wang, and W. Ma, Phys. Rev. D **74**, 115018 (2006).
- [15] G. Buchalla *et al.*, Phys. Rev. D **53**, 5185 (1996); C. T. Hill and E. H. Simmons, Phys. Rep. **381**, 235 (2003).
- [16] G. H. Wu, Phys. Rev. Lett. **74**, 4317 (1995); K. Hagiwara and N. Kitazawa, Phys. Rev. D **52**, 5374 (1995); C. X. Yue, Y. P. Kuang, and G. R. Lu, J. Phys. G **23**, 163 (1997).
- [17] J. Ellis *et al.*, Nucl. Phys. **B182**, 529 (1981); E. Eichten and K. Lane, Phys. Lett. B **90**, 125 (1980); E. Eichten *et al.*, Rev. Mod. Phys. **56**, 579 (1984).
- [18] V. A. Miransky, M. Tanabashi, and K. Yamawaki, Phys. Lett. B **221**, 177 (1989); W. A. Bardeen, C. T. Hill, and M. Lindner, Phys. Rev. D **41**, 1647 (1990); C. T. Hill, D. Kennedy, T. Onogi, and H. L. Yu, *ibid.* **47**, 2940 (1993).
- [19] C. X. Yue *et al.*, Phys. Rev. D **55**, 5541 (1997); Jinshu Huang, Zhaohua Xiong, and Gongru Lu, Commun. Theor. Phys. **37**, 709 (2002); Jinshu Huang and Gongru Lu, *ibid.* **38**, 566 (2002); G. Lv, J. S. Huang, and G. R. Lu, Phys. Rev. D **73**, 015008 (2006).
- [20] M. Bohm, H. Spiesberger, and W. Hollik, Fortschr. Phys. **34**, 687 (1986); W. Hollik, *ibid.* **38**, 165 (1990); B. Grzadkowski and W. Hollik, Nucl. Phys. **B384**, 101 (1992).
- [21] M. Clements *et al.*, Phys. Rev. D **27**, 570 (1983); A. Axelrod, Nucl. Phys. **B209**, 349 (1982); G. Passarino and M. Veltman, *ibid.* **B160**, 151 (1979).
- [22] K. M. Cheung, Phys. Rev. D **47**, 3750 (1993); H. Y. Zhou *et al.*, *ibid.* **57**, 4205 (1998); B. Zhang, Y. N. Gao, and Y. P. Kuang, *ibid.* **70**, 115012 (2004); I. Sahin, arXiv:0802.2818.
- [23] K. Hagiwara and D. Zeppenfeld, Nucl. Phys. **B313**, 560 (1989); V. Barger, T. Han, and D. Zeppenfeld, Phys. Rev. D **41**, 2782 (1990).
- [24] A. Denner, Fortschr. Phys. **41**, 307 (1994).
- [25] W. Beenakker *et al.*, Nucl. Phys. **B411**, 343 (1994).
- [26] W. M. Yao *et al.* (Particle Data Group), J. Phys. G **33**, 1 (2006).
- [27] J. Brau, Y. Okada, and N. Walker, arXiv:0712.1950; A. Djouadi *et al.*, arXiv:0709.1893; N. Phinney, N. Toge, and N. Walker, arXiv:0712.2361; T. Behnke, C. Damerell, J. Jaros, and A. Myamoto, arXiv:0712.2356.